N-Agent Ad Hoc Teamwork

Caroline Wang

Department of Computer Science The University of Texas at Austin caroline.l.wang@utexas.edu

Ishan Durugkar

Sony AI ishan.durugkar@sony.com

Arrasy Rahman

Department of Computer Science The University of Texas at Austin arrasy@cs.utexas.edu

Elad Liebman *

Amazon Science liebelad@amazon.com

Peter Stone

Department of Computer Science The University of Texas at Austin and Sony AI pstone@cs.utexas.edu

Abstract

Current approaches to learning cooperative multi-agent behaviors assume relatively restrictive settings. In standard fully cooperative multi-agent reinforcement learning, the learning algorithm controls all agents in the scenario, while in ad hoc teamwork, the learning algorithm usually assumes control over only a single agent in the scenario. However, many cooperative settings in the real world are much less restrictive. For example, in an autonomous driving scenario, a company might train its cars with the same learning algorithm, yet once on the road, these cars must cooperate with cars from another company. Towards expanding the class of scenarios that cooperative learning methods may optimally address, we introduce N-agent ad hoc teamwork (NAHT), where a set of autonomous agents must interact and cooperate with dynamically varying numbers and types of teammates. This paper formalizes the problem, and proposes the *Policy Optimization* with Agent Modelling (POAM) algorithm. POAM is a policy gradient, multi-agent reinforcement learning approach to the NAHT problem, that enables adaptation to diverse teammate behaviors by learning representations of teammate behaviors. Empirical evaluation on tasks from the multi-agent particle environment and Star-Craft II shows that POAM improves cooperative task returns compared to baseline approaches, and enables out-of-distribution generalization to unseen teammates.

1 Introduction

Advances in multi-agent reinforcement learning (MARL) [3] have enabled agents to learn solutions to various problems in zero-sum games, social dilemmas, adversarial team games, and cooperative tasks [35, 8, 18, 20, 32]. Within MARL, cooperative multi-agent reinforcement learning (CMARL) is a paradigm for learning agent teams that solve a common task via interaction with each other and the environment [21, 27, 44]. Recent CMARL methods have been able to learn impressive examples of cooperative behavior from scratch in controlled settings, where all agents are controlled by the same learning algorithm [32, 36, 4]. A related paradigm for learning cooperative behavior is ad hoc

^{*}Work was done while at SparkCognition, prior to joining Amazon.

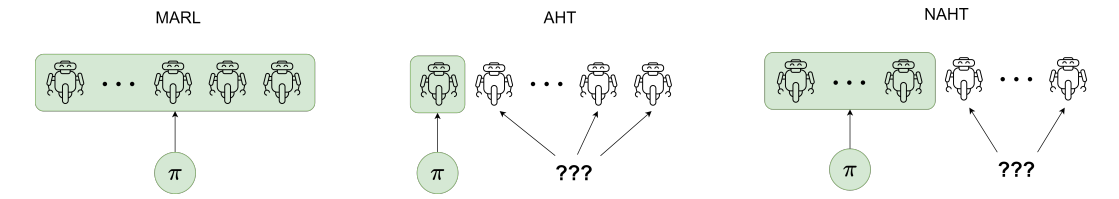


Figure 1: Left: CMARL algorithms assume full control over all M agents in a cooperative scenario. Center: AHT algorithms assume that only a single agent is controlled by the learning algorithm, while the other M-1 agents are uncontrolled and can have a diverse, unknown set of behaviors. Right: NAHT, the paradigm proposed by this paper, assumes that a potentially varying N agents are controlled by the learning algorithm, while the remaining M-N agents are uncontrolled.

teamwork (AHT). In contrast to CMARL, the objective of AHT is to create a single agent policy that can collaborate with previously unknown teammates to solve a common task [26, 37].

While a large and impressive body of work on CMARL and AHT exists, the current literature has largely examined scenarios in which either complete control over all agents is assumed, or only a single agent is adapted for cooperation [32, 36, 20, 4, 14]. Even learning methods for handling cooperative tasks in open multiagent systems [44], which encompass one of the most challenging settings where agents may enter or leave the system anytime, either operate assuming full control over all agents [16, 22] or only a single adaptive agent [30, 17, 31].

However, real-world collaborative scenarios—e.g. search-and-rescue, or robot fleets for warehouses—might demand agent *subteams* that are able to collaborate with unfamiliar teammates that follow different coordination conventions. Towards producing agent teams that are more flexible and applicable to realistic cooperative scenarios, this paper formalizes the problem setting of *N*-agent ad hoc teamwork (NAHT), in which a set of autonomous agents must interact with an uncontrolled set of teammates to perform a cooperative task. When there is only a single ad hoc agent, NAHT is equivalent to AHT. On the other hand, when all ad hoc agents are jointly trained by the same algorithm and there are no uncontrolled teammates, NAHT is equivalent to CMARL. Thus, the proposed problem setting generalizes both CMARL and AHT.

Drawing from ideas in both CMARL and AHT, we introduce Policy Optimization with Agent Modelling (POAM). POAM is a policy-gradient based approach for learning cooperative multi-agent team behaviors, in the presence of varying numbers and types of teammate behaviors. It consists of (1) an agent modeling network that generates a vector characterizing teammate behaviors, and (2) an independent actor-critic architecture, which conditions on the learned teammate vectors to enable adaptation to a variety of potential teammate behaviors. Empirical evaluation on multi-agent particle environment (MPE) and StarCraft II tasks shows that POAM learns to coordinate with a changing number of teammates of various types, with higher competency than CMARL, AHT, and naive NAHT baseline approaches. An evaluation with out-of-distribution teammates also reveals that POAM's agent modeling module improves generalization to out-of-distribution teammates, compared to baselines without agent modeling.

2 Background and Notation

The NAHT problem is formulated within the framework of **Decentralized Partially Observable Markov Decision Processes**, or Dec-POMDPs [7]. A Dec-POMDP consists of M agents, a state space \mathcal{S} , action space \mathcal{A} , per-agent observation spaces O^i , transition function $\mathcal{T}: \mathcal{S} \times \mathcal{A} \mapsto \Delta(\mathcal{S})^2$, common reward function $r: \mathcal{S} \times \mathcal{A} \mapsto \Delta(\mathbb{R})$ (thus defining a cooperative task), discount factor $\gamma \in [0,1]$ and horizon $T \in \mathbb{Z}$, which represents the maximum length of an interaction, or episode. Each agent observes the environment via its observation function, $\mathcal{O}^i: \mathcal{S} \times \mathcal{A} \mapsto \Delta(O^i)$. The state space is factored such that $\mathcal{S} = \mathcal{S}_1 \times \cdots \times \mathcal{S}_M$, where \mathcal{S}_i for $i \in \{1 \cdots M\}$ corresponds to the state space for agent i. The action space is defined analogously. Denoting H^i as its space of localized observation and action histories, agent i acts according to a policy, $\pi_i: H^i \mapsto \Delta(\mathcal{A}_i)$. In the following, we overload r to refer to both the reward function, and the task defined by that reward

 $^{^{2}\}Delta(S)$ denotes the space of probability distributions over set S.

function, whereas r_t denotes the reward at time step t. The notation -i represents all agents other than agent i.

3 NAHT Problem Formulation

Drawing from the goals of MARL and AHT [37], the goal of N-agent ad hoc teamwork is **to create a** set of autonomous agents that are able to efficiently collaborate with both known and unknown teammates to maximize return on a task. The goal is formalized below.

Let C denote a set of ad hoc agents. If the policies of the agents in C are generated by an algorithm, we say that the algorithm controls agents in C. Since our intention is to develop algorithms for generating the policies of agents in C, we refer to agents in C as *controlled*. Let U denote a set of *uncontrolled* agents, which we define as all agents in the environment not included in C.³ Following Stone et al., we assume that agents in U are not adversarially minimizing the objective of agents in C.

We model an open system of interaction, in which a random selection of M agents from sets C and U must coordinate to perform task r. For illustration, consider a warehouse staffed by robots developed by companies A and B, where there is a box-lifting task that requires three robots to accomplish. If Company A's robots are controlled agents (corresponding to C), then some robots from Company A could collaborate with robots from Company B (corresponding to U) to accomplish the task, rather than requiring that all three robots come exclusively from A or B. Motivated thus, we introduce a team sampling procedure X(U,C). At the beginning of each episode, X samples a team of M agents by first sampling N < M, then sampling N agents from the set C and M - N agents from U. We restrict consideration to teams containing at least one controlled agent, i.e $N \ge 1$. We consider X a problem parameter that is not under the control of any algorithm for generating ad hoc teammates, analogous to the transition function of the underlying Dec-POMDP. A more explicit definition of X is provided in Appendix A.1.

Without loss of generality, let $C(\theta) = \{\pi_{\theta}^i(.|s)\}_{i=1}^N$ denote a set of N controlled agent policies parameterized by θ , such that a learning algorithm might optimize for θ . Let the $\pi^{(M)}$ indicate a team of M agents and $\pi^{(M)} \sim X(U,C)$ indicate sampling such a team from U and C via the team sampling procedure. The objective of the NAHT problem is to find parameters θ , such that $C(\theta)$ maximizes the expected return in the presence of teammates from U:

$$\max_{\theta} \left(\mathbb{E}_{\boldsymbol{\pi}^{(M)} \sim X(U, C(\theta))} \left[\sum_{t=0}^{T} \gamma^{t} r_{t} \right] \right). \tag{1}$$

Challenges of the NAHT problem include: (1) coordinating with potentially unknown teammates (*generalization*), and (2) coping with a varying number of uncontrolled teammates (*openness*).

4 The Need for Dedicated NAHT Algorithms

Having introduced the NAHT problem, a natural question to consider is whether AHT solutions may optimally address NAHT problems. If so, then there would be little need to consider the NAHT problem setting. For instance, a simple yet reasonable approach consists of directly using an AHT policy to control as many agents as required in an NAHT scenario. This section illustrate the limitations of the aforementioned approach by giving a concrete example of a matrix game where (1) an AHT policy that is learned in the AHT (N=1) scenario is unlikely to do well in an NAHT scenario where N=2, and (2) even an *optimal* AHT policy is suboptimal in the N=2 setting.

Define the following simple game for M agents: at each turn, each agent a_i picks one bit $b_i \in \{0, 1\}$; at the end of each turn, all the bits are summed $s = \sum_i b_i$. The team wins if the sum of the chosen bits is exactly 1. We denote the probability of winning by P(s = 1). Suppose the uncontrolled agents

³The original AHT problem statement used the terms "known" and "unknown" agents. However, it is common for modern AHT learning methods to assume some knowledge about the "unknown" teammates during training [26]. Thus, we instead employ the terms controlled and uncontrolled.

follow a policy that independently selects 1 with probability $p = \frac{1}{M}$. In the following, we consider the three agent case, M = 3, for simplicity.

In the AHT problem setting, a learning algorithm assumes control of only a single agent. Let $p_{\rm aht}$ denote the probability with which the AHT agent selects 1. Given the aforementioned team of uncontrolled agents, we show that *any* value of $p_{\rm aht}$ results in the same P(s=1), i.e. all possible policies for the AHT agent are optimal. This occurs because the probability of winning, $P(s=1)=\frac{4}{0}$, is independent of $p_{\rm aht}$ (Lemma A.2).

Next, consider an NAHT scenario where a learning algorithm must define the actions of two out of three agents. Suppose that the same AHT policy is used to control both agents: both agents select 1 with probability $p_{\rm aht}$. Above, we demonstrated that an AHT algorithm trained in the N=1 scenario could result in learning any $p_{\rm aht}$. However, in the N=2 setting, we show that the optimal AHT policy $p_{\rm aht}=\frac{1}{3}$ and the winning probability for this policy is $P(s=1)=\frac{4}{9}$ (Lemma A.3).

Finally, we show that there exists an NAHT policy that controls both agents and obtains a higher winning probability. Consider the policy where one controlled agent always plays 0, while the other plays 1 with probability $p_{\rm naht}$. We show that the optimal $p_{\rm naht}=1$, and the probability of winning $P(s=1)=\frac{2}{3}>\frac{4}{9}$ (Lemma A.4). Thus, we have exhibited an NAHT scenario where an AHT policy that is optimal when N=1, performs worse than a simple NAHT joint policy in the N=2 setting.

5 Policy Optimization with Agent Modeling (POAM)

This section describes the proposed Policy Optimization with Agent Modeling (POAM) method to trains a collection of NAHT agents that can adaptively deal with different collections of unknown teammates. POAM relies on an agent modeling network to initially build an encoding vector of the collection of teammates encountered during an interaction. Adaptive agent policies that can maximize the controlled agents' returns are then learned by training a policy conditioned on the environment observation and team encoding vector. The training processes for agent modeling and policy networks are described in Sections 5.1 and 5.2 respectively, while an illustration of how POAM trains NAHT agents is provided in Figure 2.

5.1 Agent Modeling Network

Designing adaptive policies that enable NAHT agents to achieve optimal returns against any team of uncontrolled agents drawn from some set U, requires information on the encountered team's unknown behavior. However, in the absence of prior

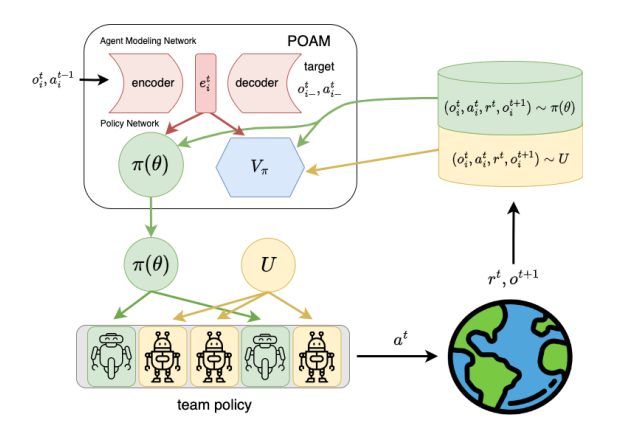


Figure 2: POAM trains a single policy network, which characterizes the behavior of all controlled agents (green), while uncontrolled agents (yellow) are drawn from U. Data from both controlled and uncontrolled agents is used to train the critic, V_{π} while the actor $\pi(\theta)$ is trained on data from the controlled agents only. The actor and critic are both conditioned on a learned team encoding vector.

knowledge about uncontrolled teammates' policies, local observations from a single timestep may not contain sufficient information regarding the encountered team. To circumvent this lack of information, POAM's agent modeling network plays a crucial role in providing *team encoding vectors* that characterize the observed behavior of teammates in the encountered team.

We identify two main criteria for desirable team encoding vectors. First, team encoding vectors should identify information regarding the unknown state and behavior of other agents in the environment (both controlled and uncontrolled). Second, team encoding vectors should ideally be computable from the sequence of local observations and actions of the team. Fulfilling both requirements

⁴Lemma A.1 shows that this is the optimal value of p for a team composed of such agents.

provides an agent with useful information for decision-making in NAHT problems, even under partial observability.

POAM produces desirable team encoding vectors by training a model with an encoder-decoder architecture, which is illustrated by red components in Figure 2. The encoder, $f_{\theta^e}^{\rm enc}: H^i \mapsto \mathbb{R}^n$, is parameterized by θ^e and processes the modeling agent's history of local observations and actions up to timestep $t, h^t = \{o_i^k, a_i^{k-1}\}_{k=1}^t$, to compute a team encoding vector, $e_i^t \in \mathbb{R}^n$. This reliance on local observations helps ensure that the agent modeling network can operate without having access to the environment state that is unavailable under partial observability. The decoder networks, $f_{\theta^o}^{\rm dec}: \mathbb{R}^n \mapsto O^{-i}$ and $f_{\theta^a}^{\rm dec}: \mathbb{R}^n \mapsto \Delta(A_{-i})$, are trained to predict the observations and actions of the modeled agents at timestep $t, (o_{-i}^t, a_{-i}^t)$, to encourage e_i^t to contain relevant information for the NAHT agents' decision-making process. Formally, this decoder is trained to minimize the following loss function to accurately predict the modeled agents' observations and actions:

$$L_{\theta^e, \theta^o, \theta^a}(h^t) = \left(||f_{\theta^o}^{\text{dec}}(f_{\theta^e}^{\text{enc}}(h^t)) - o_{-i}^t||^2 - \log(p(a_{-i}^t; f_{\theta^a}^{\text{dec}}(f_{\theta^e}^{\text{enc}}(h^t)))) \right). \tag{2}$$

5.2 Policy and Value Networks

POAM relies on an actor-critic approach to train agent policies, where the policy and critic are both conditioned on the teammate embedding described in Section 5.1.

The policy network, $\pi^i_{\theta^p}: H^i \times \mathbb{R}^n \mapsto \Delta(A_i)$, uses the NAHT agent's local observation, o^t_i , and the team embedding from the encoder network, e^t_i , to compute a policy followed by the NAHT agents. Conditioning the policy network on e^t_i allows an NAHT agent to change its behaviour based on the inferred characteristics of encountered agents. When training the policy network, we also rely on a value network $V_{\theta^c}: H^i \times \mathbb{R}^n \mapsto \mathbb{R}$, which measures the expected returns given h_t , and e^t_i . The value network serves as a baseline to reduce the variance of the gradient updates and also conditions on the learned teammate embeddings, for similar reasons to the policy.

POAM then trains the policy and value networks using an approach based off the Independent PPO algorithm [43] (IPPO). IPPO is selected as the base MARL algorithm for two reasons. First, using an independent MARL method circumvents the need to deal with the changing number of agents resulting from environment openness. Second, it has been demonstrated to be effective on various MARL tasks. POAM trains the value network to produce accurate state value estimates by minimizing the following loss function:

$$L_{\theta^c}(h^t) = \frac{1}{2} \left(V_{\theta^c}(h^t, f_{\theta^c}^{\text{enc}}(h^t)) - \hat{V}^t \right)^2, \tag{3}$$

where $\hat{V}^t = \sum_{l=0}^T \gamma^l r^{t+l}$. The policy network is trained to minimize the PPO loss function [34].

Leveraging data from uncontrolled agents In the NAHT setting, we assume access to the *joint* observations and actions generated by the current team deployed in the environment, where the team consists of a mix of controlled and uncontrolled agents. POAM leverages data from both controlled and uncontrolled agents to train the value network—in effect, treating the uncontrolled agents as exploration policies. This aspect of POAM is a significant departure from PPO, which is a fully on-policy algorithm. However, only data from the controlled agents is used to train the policy network, as the policy update is highly sensitive to off-policy data.

6 Experiments and Results

This section presents an empirical evaluation of POAM and baseline approaches across different NAHT problems. We investigate three questions and foreshadow the conclusions:

Q1: Does POAM lead to better sample efficiency and/or asymptotic return than baselines? (Usually)

Q2: Can we verify that the two key ideas of POAM—agent modelling and use of data from uncontrolled agents—work as desired and contribute positively towards POAM's performance? (Yes)

O3: Does agent modelling improve generalization to previously unseen teammates? (Yes)

Full implementation details, including all hyperparameter values, along with additional empirical results, appear in Appendix. Our code is included with the submission and will be open-sourced upon publication.

6.1 Experimental Design

This subsection describes the experimental design, including the particular NAHT problem setting, training procedure, experimental domain, and baselines.

A Practical Instantiation of NAHT Similarly to AHT, the NAHT problem can be parameterized by the amount of knowledge that controlled agents have about uncontrolled agents, and whether uncontrolled agents can adapt to the behavior of controlled agents [5]. Furthermore, as a direct result of the fact that an NAHT algorithm may control more than a single agent, the NAHT problem may also be parameterized by whether the controlled agents are homogeneous, whether they can communicate, and what the team sampling procedure is. While the fully general problem setting allows for heterogeneous, communicating, controlled agents that have no knowledge of the uncontrolled agents, as a first step, this paper focuses on a special case of the NAHT problem, where agents are homogeneous, non-communicating, may learn about uncontrolled agents via interaction, and where the team sampling procedure consists of a uniform random sampling scheme from U and C (see Appendix A.3.1 for details). This case is designed primarily to assess whether controlled subteams may outperform independent controlled agents, when cooperating with multiple types of uncontrolled agents. We leave consideration of broader NAHT scenarios for future work.

Generating Uncontrolled Teammates To generate a set of uncontrolled teammates U, the following MARL algorithms are used to train agent teams: VDN [39], QMIX [32], IQL [40], IPPO, and MAPPO [43]. We verify that the generated team behaviors are diverse by checking that (1) teams trained by the same algorithm learn non-compatible coordination conventions, and (2) teams trained by different algorithms are not compatible (Appendix A.4). This emergence of diverse teammate behaviors from training agents using different MARL algorithms under different seeds aligns with the findings from Strouse et al. [38].

Let U_{train} denote the set of uncontrolled teammates used to train POAM and the baseline methods. U_{train} consists of five teams, where each individual team is trained via VDN, QMIX, IQL, IPPO and MAPPO, respectively. U_{test} consists of a set of holdout teams trained via the same MARL algorithms, but that have not been seen during training. The experimental results reported in 6.2 and 6.3 are computed with respect to U_{train} only, while the experimental results in 6.4 use U_{test} .

Experimental Domains Experiments are conducted on a predator-prey mpe-pp task implemented within the multi-agent particle environment [23], and the 5v6, 8v9, 10v11, 3s5z tasks from the StarCraft Multi-Agent Challenge (SMAC) benchmark [33]. On the mpe-pp task, three predators must cooperatively pursue a pretrained prey agent. The team receives a reward of +1 per time step that two or more predators collide with the prey. On the SMAC tasks, a team of allied agents must defeat a team of enemy agents controlled by the game server. For each task, the first number in the task name indicates the number of allied agents, while the second indicates the number of enemy agents. The team is rewarded for defeating enemies, with a large bonus for defeating all enemies. See Appendix A.3.2 for full details.

Baselines As NAHT is a new problem proposed by this paper, there are no prior algorithms that are directly designed for the NAHT problem. Therefore, we construct three baselines to contextualize the performance of POAM. All methods employ full parameter sharing [29].

- *Naive MARL*: various well-known MARL algorithms are considered, including both independent and centralized training with decentralized execution algorithms [13]. The algorithms evaluated here include IQL [10], VDN [39], QMIX [32], IPPO, and MAPPO [43]. The MARL baselines are trained in self-play and then evaluated in the NAHT setting. In the following, only the performance of the *best* naive MARL baseline is reported.
- Independent PPO in the NAHT setting (IPPO-NAHT): IPPO is a policy gradient MARL algorithm that directly generalizes PPO [34] to the multi-agent setting. It was found to be surprisingly effective on a variety of MARL benchmarks [43]. In contrast to the naive MARL baselines, IPPO-NAHT is trained using the NAHT training scheme presented in Section 6.1. The variant considered here employs full parameter sharing, where the actor is trained on data only from controlled agents, but the critic is trained using data from both controlled and uncontrolled agents. The latter detail is a key algorithmic feature which POAM also employs, but is an extension from the most naive

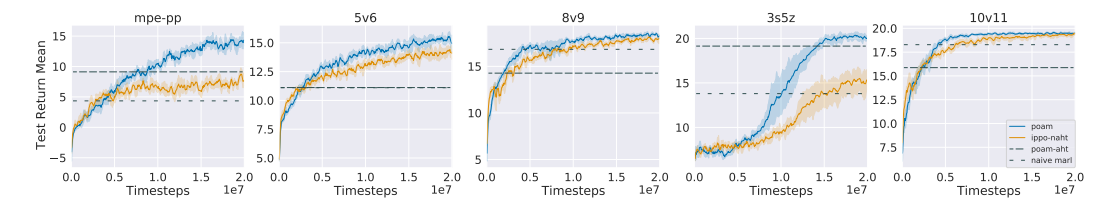


Figure 3: POAM consistently improves over the baselines of IPPO-NAHT, POAM-AHT, and the best naive MARL baseline in all tasks, in either sample efficiency or asymptotic return. Results are computed over three trials, while the shaded region represents the 95% confidence interval.

version of PPO (see Section 6.3). IPPO can be considered an ablation of POAM, where the agent modeling module is removed.

• POAM in the AHT setting (POAM-AHT): As considered in Section 4, a natural baseline approach to the NAHT problem is use AHT algorithms that train only a single controlled agent, and copy these policies as many times as needed in the NAHT setting. To evaluate the intuition that AHT policies do not suffice for the NAHT problem setting, we consider an AHT version of POAM that is trained identically to POAM, but where the number of controlled agents N=1 during training.

6.2 Main Results

This section addresses Q1—that is, whether POAM improves asymptotic return and/or sample efficiency, compared to baselines. Figure 3 shows the learning curves of POAM and IPPO-NAHT, and the test returns achieved by the best naive MARL baseline and POAM-AHT, on all tasks. ⁵ All learning curves consist of the mean test returns across three trials, while the shaded regions reflect the 95% confidence intervals.

We find that for all tasks, POAM outperforms baselines in terms of asymptotic return for three out of five tasks (pp, 5v6, 3s5z). For all tasks, POAM's initial sample efficiency is similar to that of IPPO-NAHT for the first few million steps of training, after which POAM displays higher return. We attribute this to the initial costs incurred by learning team encoding vectors, which once learned, improves learning efficiency. IPPO-NAHT, which can be viewed as an ablation of POAM with no agent modeling, is the next best performing method. Although IPPO-NAHT has generally poorer sample efficiency than POAM, the method converges to approximately the same returns on two out of five tasks (8v9 and 10v11). While the agent modeling module of POAM provides team embedding vectors to the policy learning process, the embeddings are themselves produced from each agent's own observation. Since no additional information is provided to POAM agents, it is unsurprising that IPPO-NAHT can converge to similar solutions as POAM, given enough training steps.

Finally, while the best naive MARL baseline and POAM-AHT learn good solutions on some tasks, neither method consistently performs well across all tasks. Overall, POAM discovers the most consistently performant policies compared to baseline methods, in a sample-efficient manner. We conclude that (1) agent modeling improves learning efficiency, and (2) direct duplication of AHT-trained policies is less effective than methods that co-train agents for NAHT.

6.3 A Closer Look at POAM

Two key aspects of POAM are the use of a recurrent teammate modeling module, and the use of data from uncontrolled agents to train the critic (Q2). We perform further analysis

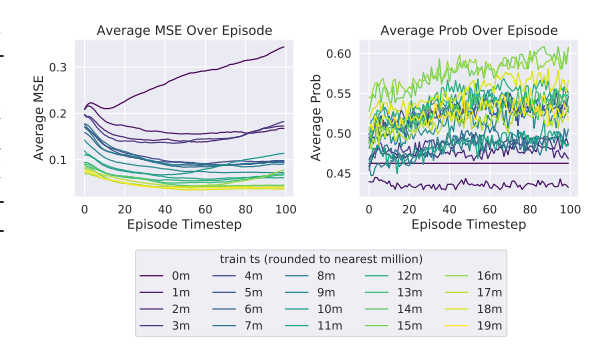


Figure 4: Evolution of the within-episode mean squared error (left) and the within-episode probability of actions of modelled teammates (right), computed by the POAM agent over the course of training on the mpe-pp task.

⁵See the Appendix for tables providing the performances of all naive MARL methods, across all tasks.

of both aspects on the mpe-pp and 5v6 tasks; results on 5v6 may be found in Appendix A.4.

Teammate modeling performance In the NAHT training/evaluation setting, a new set of teammates is sampled at the beginning of each episode. Therefore, an important subtask for a competent NAHT agent is to rapidly model the distribution and type of teammates at the beginning of the episode, to enable the policy to exploit that knowledge as the episode progresses. This task is especially challenging in the presence of partial observability (a property of the SMAC tasks). To address the above challenges, POAM employs a recurrent encoder, which encodes the POAM agent's history of observations and actions to an embedding vector, and a (non-recurrent) decoder network, which predicts the egocentric observations and actions for all teammates.

A natural question then, is whether the learned teammate encoding vectors actually improve over the course of an episode. Figures 4 and 8 depict the within-episode *mean squared error* (MSE) of the observation predicted by the decoder, and the within-episode *probability* of the action actually taken by the modelled teammates, according to the decoder's modelled action distribution. Each curve corresponds to a different training checkpoint of a single run.

For both tasks, we observe that the average MSE decreases over the course of training, while the average probability of the taken actions increases. For later training checkpoints, we observe that the average MSE actually decreases *within* an episode, while the average probability increases. This reflects the increased confidence of the agent modelling module, as more data is observed about teammates. Thus, we conclude that POAM is able to cope with the challenges introduced by the sampled teammates and partial observability, to learn accurate teamate models.

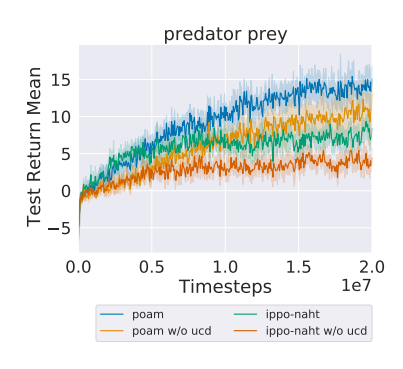


Figure 5: Learning curves of POAM and IPPO, where the value network is trained with and without uncontrolled agents' data (UCD).

Impact of data from non-controlled agents Recall that both POAM and IPPO-NAHT update the value network using data from both the controlled and uncontrolled agents. As Figures 5 and 9 show, this algorithmic feature results in a significant performance gain over training using on-policy data only, for both POAM and IPPO-NAHT.

6.4 Out of Distribution Generalization

The AHT literature commonly assumes that some subset of the uncontrolled teammates of interest may be interacted directly with during training [28, 6, 30]. Experiments in the previous sections were conducted under this assumption. This section conducts an analysis of how POAM performs when this assumption is relaxed—that is, when the teammates have not been seen previously (Q3). The out-of-distribution (OOD) teammate setting is of interest because in realistic scenarios, it may be challenging to enumerate all teammates likely to be encountered in the wild. Here, OOD teammates are generated

by using MARL algorithms with different random seeds to generate teammates that have not been interacted with during training.

Figures 6 and 10 shows the mean and standard error of the test return achieved by POAM, compared to IPPO-NAHT, when the algorithm in question is paired with previously unseen seeds of IPPO, IQL, MAPPO, QMIX, and VDN In three out of five tasks (mpe, 5v6, 3s5z), POAM has a significantly higher return than IPPO-NAHT, while the remaining two tasks exhibit a smaller improvement. For all tasks, we observe that the std. error for POAM is lower than that of IPPO-NAHT, showing that POAM performs more consistently against a range of teammates and team configurations than IPPO-NAHT.

7 Related Works

This section summarizes related work in the areas most closely related to NAHT, namely, ad hoc teamwork, zero-shot coordination, agent modeling, and cooperative MARL.

Ad Hoc Teamwork & Zero-Shot Coordination. Prior works in ad hoc teamwork [37] and zero-shot coordination (ZSC) [15] explored methods to design adaptive agents that can optimally collaborate with unknown teammates. While they both highly resemble the NAHT problem, existing methods for AHT [30, 26] and ZSC [15, 24] have been limited to single-agent control scenarios. We argue that direct, naive applications of AHT and ZSC techniques to our problem of interest are ineffective—see the discussion in Section 4 and results in Section 6.

Recent research in AHT and ZSC utilizes neural networks to improve agent collaboration within various team configurations. These recent works mostly focus on two approaches. The first approach trains the agent to adapt to unknown teammates by characterizing teammates' behavior as fixed-length vectors using neural networks and learning a policy network conditioned ing neural networks and learning a policy network conditioned on these vectors [30, 28, 45]. The second designs teammate policies that maximize the agent's performance when collaborating with diverse teammates [24, 30]. Which is now improved generalization to control multiple agents amid the existence of unknown teammates. While

this also offers a potential path for robust NAHT agents, designing teammate policies for training will be kept as future work.

Mean Test 5.0 ippo-naht 2.5 ippo mappo qmix Target Algorithms Figure 6: Mean and standard error of test returns achieved by POAM and IPPO-NAHT, when paired

15.0

Return 10.0

7.5

OOD Evaluation: Predator Prey

Evaluating Agents' Cooperative Capabilities. Beyond training agents to collaborate with teammates having unknown policies, researchers have developed environments and metrics to assess cooperative abilities. The Melting Pot suite [19, 1] mostly evaluates controlled agents' ability to maximize utilitarian welfare against unknown agents. However, this evaluation suite focuses on mixed-motive games where agents may have conflicting goals. This contrasts with our work's scope of fully cooperative settings, where all agents share the same reward function. MacAlpine et al. [25] also explored alternative metrics to measure agents' cooperative capabilities while disentangling the effects of their overall skills in drop-in RoboSoccer.

Agent Modeling. Agent modeling [2] helps us characterize other agents based on their actions. Such characterizations could attempt to infer important attributes of another agent's decision making process such as their goals [12] or policies [28]. POAM and most existing AHT techniques rely on agent modeling to provide important teammate information for decision-making when collaborating with unknown teammates.

Cooperative MARL. Cooperative Multi-Agent Reinforcement Learning (MARL) explores algorithms for training agent teams on fully cooperative tasks. Some existing methods focus on credit assignment and decentralized control [11, 32]. Other works in cooperative MARL also leverage parameter sharing and role assignment (e.g., [9, 42]) to decide an optimal division of labor between agents. However, these techniques assume control over all existing agents during training and evaluation. This limits these techniques' effectiveness in settings with new teammates (NAHT problem) as shown in prior work [41, 15, 30].

Conclusion

This paper proposes and formulates the problem of N-agent ad hoc teamwork (NAHT), a generalization of both AHT and MARL. It further proposes a multi-agent reinforcement learning algorithm to train NAHT agents called POAM, and develops a procedure to train and evaluate NAHT agents. POAM is a policy gradient approach that uses an encoder-decoder architecture to perform teammate modeling, and leverages data from uncontrolled agents for policy optimization. Empirical validation on MPE and StarCraft II tasks shows that POAM consistently improves over baseline methods that naively apply existing MARL and AHT approaches, in terms of sample efficiency, asymptotic return, and generalization to out-of-distribution teammates.

Limitations and Future Work. This paper addresses a special case of the NAHT problem, with homogeneous and non-communicating agents. POAM, which employs full parameter sharing, may not perform well in settings with heterogeneous agents, or in settings that require highly differentiated roles. POAM also does not leverage centralized state information or allow communication between controlled agents. Incorporating this information might enable learning improved NAHT policies. Further, POAM's actor update is purely on-policy, and therefore cannot leverage data generated by uncontrolled agents. Future work may consider off-policy learning methods as a solution strategy. In addition to the directions suggested by POAM's limitations, algorithmic ideas from AHT, such as diversity-based teammate generation [24] and teammate-model-based planning methods [6], also suggest rich avenues for future work. Having introduced the NAHT problem in this work, we hope the community explores the many potential directions to design even better NAHT algorithms by considering advances in MARL, AHT and agent modeling.

References

- [1] John P Agapiou, Alexander Sasha Vezhnevets, Edgar A Duéñez-Guzmán, Jayd Matyas, Yiran Mao, Peter Sunehag, Raphael Köster, Udari Madhushani, Kavya Kopparapu, Ramona Comanescu, et al. Melting pot 2.0. *arXiv preprint arXiv:2211.13746*, 2022.
- [2] Stefano V Albrecht and Peter Stone. Autonomous agents modelling other agents: A comprehensive survey and open problems. *Artificial Intelligence*, 258:66–95, 2018.
- [3] Stefano V. Albrecht, Filippos Christianos, and Lukas Schäfer. *Multi-Agent Reinforcement Learning: Foundations and Modern Approaches*. MIT Press, 2024. URL https://www.marl-book.com.
- [4] Bowen Baker, Ingmar Kanitscheider, Todor Markov, Yi Wu, Glenn Powell, Bob McGrew, and Igor Mordatch. Emergent Tool Use From Multi-Agent Autocurricula. In *International Conference on Learning Representations*, September 2019. URL https://openreview.net/forum?id=SkxpxJBKwS.
- [5] Samuel Barrett and Peter Stone. An analysis framework for ad hoc teamwork tasks. In *Proceedings of the 11th International Conference on Autonomous Agents and Multiagent Systems-Volume 1*, pages 357–364, 2012.
- [6] Samuel Barrett, Avi Rosenfeld, Sarit Kraus, and Peter Stone. Making friends on the fly: Cooperating with new teammates. *Artificial Intelligence*, 242:132–171, January 2017. ISSN 0004-3702. doi: 10.1016/j.artint.2016.10.005. URL https://www.sciencedirect.com/science/article/pii/S0004370216301266.
- [7] Daniel S. Bernstein, Robert Givan, Neil Immerman, and Shlomo Zilberstein. The Complexity of Decentralized Control of Markov Decision Processes. *Mathematics of Operations Research*, 27(4):819–840, November 2002. ISSN 0364-765X. doi: 10.1287/moor.27.4.819.297. URL https://pubsonline.informs.org/doi/10.1287/moor.27.4.819.297.
- [8] Noam Brown and Tuomas Sandholm. Superhuman ai for heads-up no-limit poker: Libratus beats top professionals. *Science*, 359(6374):418–424, 2018. doi: 10.1126/science.aao1733. URL https://www.science.org/doi/abs/10.1126/science.aao1733.
- [9] Filippos Christianos, Georgios Papoudakis, Muhammad A Rahman, and Stefano V Albrecht. Scaling multi-agent reinforcement learning with selective parameter sharing. In *International Conference on Machine Learning*, pages 1989–1998. PMLR, 2021.
- [10] Caroline Claus and Craig Boutilier. The dynamics of reinforcement learning in cooperative multiagent systems. In *Proceedings of the fifteenth national/tenth conference on Artificial* intelligence/Innovative applications of artificial intelligence, AAAI '98/IAAI '98, pages 746– 752, USA, July 1998. American Association for Artificial Intelligence. ISBN 978-0-262-51098-1.
- [11] Jakob Foerster, Gregory Farquhar, Triantafyllos Afouras, Nantas Nardelli, and Shimon Whiteson. Counterfactual multi-agent policy gradients. In *Proceedings of the AAAI conference on artificial intelligence*, volume 32, 2018.
- [12] Josiah P Hanna, Arrasy Rahman, Elliot Fosong, Francisco Eiras, Mihai Dobre, John Redford, Subramanian Ramamoorthy, and Stefano V Albrecht. Interpretable goal recognition in the presence of occluded factors for autonomous vehicles. In 2021 IEEE/RSJ International Conference on Intelligent Robots and Systems (IROS), pages 7044–7051. IEEE, 2021.

- [13] Pablo Hernandez-Leal, Bilal Kartal, and Matthew E. Taylor. A Survey and Critique of Multiagent Deep Reinforcement Learning. *Autonomous Agents and Multi-Agent Systems*, 33(6):750–797, November 2019. ISSN 1387-2532, 1573-7454. doi: 10.1007/s10458-019-09421-1. URL http://arxiv.org/abs/1810.05587. arXiv:1810.05587 [cs].
- [14] Hengyuan Hu and Jakob N. Foerster. Simplified Action Decoder for Deep Multi-Agent Reinforcement Learning. September 2019. URL https://openreview.net/forum?id=B1xm3RVtwB.
- [15] Hengyuan Hu, Adam Lerer, Alex Peysakhovich, and Jakob Foerster. "other-play" for zero-shot coordination. In *International Conference on Machine Learning*, pages 4399–4410. PMLR, 2020.
- [16] Jiechuan Jiang, Chen Dun, Tiejun Huang, and Zongqing Lu. Graph convolutional reinforcement learning. In *International Conference on Learning Representations*, 2019.
- [17] Anirudh Kakarlapudi, Gayathri Anil, Adam Eck, Prashant Doshi, and Leen-Kiat Soh. Decision-theoretic planning with communication in open multiagent systems. In *Uncertainty in Artificial Intelligence*, pages 938–948. PMLR, 2022.
- [18] Raphael Koster, Miruna Pîslar, Andrea Tacchetti, Jan Balaguer, Leqi Liu, Romuald Elie, Oliver P Hauser, Karl Tuyls, Matt Botvinick, and Christopher Summerfield. Using deep reinforcement learning to promote sustainable human behaviour on a common pool resource problem, 2024. URL https://arxiv.org/ftp/arxiv/papers/2404/2404.15059.pdf.
- [19] Joel Z Leibo, Edgar A Dueñez-Guzman, Alexander Vezhnevets, John P Agapiou, Peter Sunehag, Raphael Koster, Jayd Matyas, Charlie Beattie, Igor Mordatch, and Thore Graepel. Scalable evaluation of multi-agent reinforcement learning with melting pot. In *International conference* on machine learning, pages 6187–6199. PMLR, 2021.
- [20] Fanqi Lin, Shiyu Huang, Tim Pearce, Wenze Chen, and Wei-Wei Tu. TiZero: Mastering Multi-Agent Football with Curriculum Learning and Self-Play. In *Proceedings of the 2023 International Conference on Autonomous Agents and Multiagent Systems*, AAMAS '23, pages 67–76, Richland, SC, May 2023. International Foundation for Autonomous Agents and Multiagent Systems. ISBN 978-1-4503-9432-1.
- [21] Michael L Littman. Markov games as a framework for multi-agent reinforcement learning. In *Machine learning proceedings 1994*, pages 157–163. Elsevier, 1994.
- [22] Bo Liu, Qiang Liu, Peter Stone, Animesh Garg, Yuke Zhu, and Anima Anandkumar. Coach-player multi-agent reinforcement learning for dynamic team composition. In *International Conference on Machine Learning*, pages 6860–6870. PMLR, 2021.
- [23] Ryan Lowe, Yi Wu, Aviv Tamar, Jean Harb, Pieter Abbeel, and Igor Mordatch. Multi-agent actor-critic for mixed cooperative-competitive environments. *Neural Information Processing Systems (NIPS)*, 2017.
- [24] Andrei Lupu, Brandon Cui, Hengyuan Hu, and Jakob Foerster. Trajectory diversity for zero-shot coordination. In *International conference on machine learning*, pages 7204–7213. PMLR, 2021.
- [25] Patrick MacAlpine and Peter Stone. Evaluating ad hoc teamwork performance in drop-in player challenges. In Gita Sukthankar and Juan A. Rodriguez-Aguilar, editors, *Autonomous Agents and Multiagent Systems*, *AAMAS 2017 Workshops*, *Best Papers*, pages 168–186. Springer International Publishing, 2017. URL http://nn.cs.utexas.edu/?LNAI17-MacAlpine.
- [26] Reuth Mirsky, Ignacio Carlucho, Arrasy Rahman, Elliot Fosong, William Macke, Mohan Sridharan, Peter Stone, and Stefano V Albrecht. A survey of ad hoc teamwork research. In *European Conference on Multi-Agent Systems*, pages 275–293. Springer, 2022.
- [27] Liviu Panait and Sean Luke. Cooperative multi-agent learning: The state of the art. *Autonomous Agents and Multi-Agent Systems*, 11:387–434, 2005. URL https://api.semanticscholar.org/CorpusID:19706.

- [28] Georgios Papoudakis, Filippos Christianos, and Stefano V. Albrecht. Agent modelling under partial observability for deep reinforcement learning. In *Advances in Neural Information Processing Systems*, 2021.
- [29] Georgios Papoudakis, Filippos Christianos, Lukas Schäfer, and Stefano V. Albrecht. Benchmarking Multi-Agent Deep Reinforcement Learning Algorithms in Cooperative Tasks. In Advances in Neural Information Processing Systems, volume 34, 2021.
- [30] Arrasy Rahman, Niklas Höpner, Filippos Christianos, and Stefano V. Albrecht. Towards Open Ad Hoc Teamwork Using Graph-based Policy Learning. In *Proceedings of the 38 th International Conference on Machine Learning*, volume 139. PMLR, June 2021.
- [31] Arrasy Rahman, Ignacio Carlucho, Niklas Höpner, and Stefano V. Albrecht. A general learning framework for open ad hoc teamwork using graph-based policy learning. *Journal of Machine Learning Research*, 24(298):1–74, 2023. URL http://jmlr.org/papers/v24/22-099.html.
- [32] Tabish Rashid, Mikayel Samvelyan, Christian Schroeder, Gregory Farquhar, Jakob Foerster, and Shimon Whiteson. QMIX: Monotonic value function factorisation for deep multi-agent reinforcement learning. In *Proceedings of the 35th International Conference on Machine Learning*, volume 80 of *Proceedings of Machine Learning Research*. PMLR, 2018.
- [33] Mikayel Samvelyan, Tabish Rashid, Christian Schroeder de Witt, Gregory Farquhar, Nantas Nardelli, Tim G. J. Rudner, Chia-Man Hung, Philiph H. S. Torr, Jakob Foerster, and Shimon Whiteson. The StarCraft Multi-Agent Challenge. *CoRR*, abs/1902.04043, 2019.
- [34] John Schulman, Filip Wolski, Prafulla Dhariwal, Alec Radford, and Oleg Klimov. Proximal policy optimization algorithms. *ArXiv*, abs/1707.06347, 2017. URL https://api.semanticscholar.org/CorpusID:28695052.
- [35] David Silver, Aja Huang, Chris J Maddison, Arthur Guez, Laurent Sifre, George Van Den Driessche, Julian Schrittwieser, Ioannis Antonoglou, Veda Panneershelvam, Marc Lanctot, et al. Mastering the game of go with deep neural networks and tree search. *nature*, 529(7587):484–489, 2016.
- [36] Kyunghwan Son, Daewoo Kim, Wan Ju Kang, David Earl Hostallero, and Yung Yi. QTRAN: Learning to Factorize with Transformation for Cooperative Multi-Agent Reinforcement Learning. In *Proceedings of the 36th International Conference on Machine Learning*, pages 5887–5896. PMLR, May 2019. URL https://proceedings.mlr.press/v97/son19a.html.
- [37] Peter Stone, Gal Kaminka, Sarit Kraus, and Jeffrey Rosenschein. Ad Hoc Autonomous Agent Teams: Collaboration without Pre-Coordination. In *Proceedings of the AAAI Conference on Artificial Intelligence*, volume 24, pages 1504–1509, July 2010. doi: 10.1609/aaai.v24i1.7529. URL https://ojs.aaai.org/index.php/AAAI/article/view/7529.
- [38] DJ Strouse, Kevin McKee, Matt Botvinick, Edward Hughes, and Richard Everett. Collaborating with Humans without Human Data. In M. Ranzato, A. Beygelzimer, Y. Dauphin, P. S. Liang, and J. Wortman Vaughan, editors, *Advances in Neural Information Processing Systems*, volume 34, pages 14502–14515, 2021. URL https://proceedings.neurips.cc/paper_files/paper/2021/file/797134c3e42371bb4979a462eb2f042a-Paper.pdf.
- [39] Peter Sunehag, Guy Lever, Audrunas Gruslys, Wojciech Marian Czarnecki, Vinicius Zambaldi, Max Jaderberg, Marc Lanctot, Nicolas Sonnerat, Joel Z. Leibo, Karl Tuyls, and Thore Graepel. Value-decomposition networks for cooperative multi-agent learning based on team reward. In Proceedings of the 17th International Conference on Autonomous Agents and Multi Agent Systems, AAMAS '18, 2018.
- [40] Ming Tan. Multi-agent reinforcement learning: Independent versus cooperative agents. In *International Conference on Machine Learning*, 1997. URL https://api.semanticscholar.org/CorpusID:267858156.
- [41] Alexander Vezhnevets, Yuhuai Wu, Maria Eckstein, Rémi Leblond, and Joel Z Leibo. Options as responses: Grounding behavioural hierarchies in multi-agent reinforcement learning. In *International Conference on Machine Learning*, pages 9733–9742. PMLR, 2020.

- [42] Mingyu Yang, Jian Zhao, Xunhan Hu, Wengang Zhou, Jiangcheng Zhu, and Houqiang Li. Ldsa: Learning dynamic subtask assignment in cooperative multi-agent reinforcement learning. *Advances in Neural Information Processing Systems*, 35:1698–1710, 2022.
- [43] Chao Yu, Akash Velu, Eugene Vinitsky, Yu Wang, Alexandre Bayen, and Yi Wu. The surprising effectiveness of mappo in cooperative multi-agent games. In *Proceedings of the Neural Information Processing Systems Track on Datasets and Benchmarks*, 2022.
- [44] Lei Yuan, Ziqian Zhang, Lihe Li, Cong Guan, and Yang Yu. A survey of progress on cooperative multi-agent reinforcement learning in open environment. *arXiv preprint arXiv:2312.01058*, 2023.
- [45] Luisa Zintgraf, Sam Devlin, Kamil Ciosek, Shimon Whiteson, and Katja Hofmann. Deep interactive bayesian reinforcement learning via meta-learning. arXiv preprint arXiv:2101.03864, 2021

A Appendix

A.1 An Example of the Team Sampling Procedure

Let $g(k,\mu,s)$ represent a function for randomly selecting k elements from a generic set μ , conditioned on a state $s \in \mathcal{S}$. For instance, g might be the distribution, $Multinomial(k,|\mu|,\phi(s))$, for selecting k elements with replacement from the set μ , parameterized by the state-dependent probability logits $\phi(s) \in [0,1]^{|\mu|}$. Allowing g to depend on an initial state enriches the representable open interactions. Returning to our robot warehouse example, a state-dependent g might enable us to model that robots suitable for heavy loads are more likely to be present near the loading dock area. Similarly, if the time is included in the state, we would be able to model dynamic characteristics, e.g. that certain types of robots are only available during regular working hours, when humans are available to supervise. Of course, in simple cases, g might be state-independent. For $s \in \mathcal{S}$, X is a sampling procedure parameterized by the tuple $(s, M, U, C, \phi_M, g_U, g_C)$, where $\phi_M \in [0, 1]^M$ represents the logits of a categorical distribution:

- 1. Sample an integer N from $Cat(\phi_M)$.
- 2. Sample N controlled agents via g_U from U.
- 3. Sample M-N uncontrolled agents via g_C from C.

Note that the agent sampling functions g_U , g_C could employ sampling with replacement to model scenarios where two robots may use the same policy, or sampling without replacement for scenarios where that is not possible (e.g. if all robots are heterogeneous).

A.2 Further Discussion of the Motivating Example

This section provides proofs for claims in Section 4, and further discussion in support of the motivating example.

Lemma A.1. For a team of M agents independently and identically selecting actions with probability p, the p that maximizes the probability of winning is $p = \frac{1}{M}$.

Proof. The probability of winning, P(s = 1) may be computed as follows:

$$P(s=1) = M * P(\text{agent } i \text{ chooses } 1 \text{ and } i^- \text{ choose } 0) = Mp(1-p)^{M-1}$$
.

We wish to analytically compute the global maxima of this expression with respect to p, by considering the boundary points $p \in 0, 1$ and the zeros of the first derivative.

Clearly, if all agents select 1 with probability 0, the team cannot win; thus, p=0 is not a maxima. Similarly, if all agents select 1 with probability 1, the team also never wins; thus, p=1 is also not a maxima. Next, we compute the derivative of P(s=1):

$$\frac{d[P(s=1)]}{dp} = M[(1-p)^{M-1} - (M-1)p(1-p)^{M-2}]$$
$$= M[(1-p)^{M-2}[(1-p) - (M-1)p]].$$

The zeros of the above expression occur at p=0 and $p=\frac{1}{M}$. For $p=\frac{1}{M}$, note that $P(s=1)=(\frac{M-1}{M})^{M-1}>0$; thus, $p=\frac{1}{M}$ must be the global maximum.

Lemma A.2. In a team of three agents consisting of two uncontrolled agents who select 1 with probability $p = \frac{1}{3}$, and one controlled ad hoc agent who selects 1 with probability p_{aht} , the probability of winning is $P(s = 1) = \frac{4}{9}$.

Proof. Let s_u denote the sum of the bits chosen by the two uncontrolled agents, and b_{aht} denote the bit value chosen by the controlled agent. The probability of winning can be computed by partitioning the winning outcomes by whether $s_u=1$ and the ad hoc agent selects 0, or whether the ad hoc agent selects 1 and both uncontrolled agents select 0, $s_u=0$.

$$\begin{split} P(s=1) &= P(s_u = 1 \wedge b_{aht} = 0) + P(s_u = 0 \wedge b_{aht} = 1) \\ &= 2 \cdot \frac{1}{3} \cdot \frac{2}{3} \cdot \left(1 - p_{\text{aht}}\right) + p_{\text{aht}} \left(\frac{2}{3} \cdot \frac{2}{3}\right) \\ &= \frac{4}{9} - \frac{4}{9} \cdot p_{\text{aht}} + \frac{4}{9} \cdot p_{\text{aht}} \\ &= \frac{4}{9}. \end{split}$$

Lemma A.3. In a team of three agents where two ad hoc agents select 1 with probability p_{aht} and the remaining uncontrolled agent selects 1 with probability $\frac{1}{3}$, the maximizing $p_{aht} = \frac{1}{3}$ and the corresponding winning probability is $P(s=1) = \frac{4}{9}$.

Proof. Let s_{aht} denote the sum of the bits chosen by the two ad hoc agents, and b_u denote the bit value chosen by the uncontrolled agent. The probability of winning may be directly computed as follows:

$$\begin{split} P(s=1) &= P(s_{aht} = 1 \wedge a_u = 0) + P(s_{aht} = 0 \wedge a_u = 1) \\ &= 2 \cdot p_{\text{aht}} \cdot (1 - p_{\text{aht}}) \cdot \frac{2}{3} + (1 - p_{\text{aht}})^2 \cdot \frac{1}{3} \\ &= (1 - p_{\text{aht}}) \left[\frac{4}{3} p_{\text{aht}} + \frac{1}{3} (1 - p_{\text{aht}}) \right] \\ &= (1 - p_{\text{aht}}) \left(\frac{1}{3} + p_{\text{aht}} \right). \end{split}$$

To determine the maximizing value, we compute P(s=1) at the boundary points $p_{\text{aht}} \in \{0,1\}$ and at the zeros of the derivative of P(s=1). Note that for $p_{\text{aht}} = 0$, $P(s=1) = \frac{1}{3}$, while for $p_{\text{aht}} = 1$, P(s=1) = 0.

The derivative of the analytic expression of P(s = 1) with respect to p_{aht} is:

$$\frac{d[P(s=1)]}{dp_{\text{aht}}} = (1 - p_{\text{aht}}) - \left(\frac{1}{3} + p_{\text{aht}}\right) = \frac{2}{3} - 2p_{\text{aht}}.$$
 (4)

The zeros of the above expression occur at $p_{\text{aht}} = \frac{1}{3}$, which corresponds to $P(s=1) = \frac{4}{9}$.

Lemma A.4. In a team of three agents where one agent always selects 0, one agent selects 1 with probability $\frac{1}{3}$, and the last agent selects 1 with probability p_{naht} , the optimal $p_{naht} = 1$ and results in a winning probability of $P(s = 1) = \frac{2}{3}$.

Proof. Since one of the two controlled agents always plays 0, the game effectively becomes a two-player game instead.

Let a_u denote the action selected by the uncontrolled agent, and let a_{naht} denote the action of the controlled agent. The probability of winning may be directly computed as follows:

$$\begin{split} P(s=1) &= P(a_u = 1 \wedge a_{naht} = 0) + P(a_u = 0 \wedge a_{naht} = 1) \\ &= \frac{1}{3} \cdot (1 - p_{\text{naht}}) + \frac{2}{3} \cdot p_{\text{naht}} \\ &= \frac{1}{3} + \frac{1}{3} \cdot p_{\text{naht}}. \end{split}$$

It is clear that $p_{\text{naht}}=1$ maximizes P(s=1), and the corresponding value of $P(s=1)=\frac{2}{3}$.

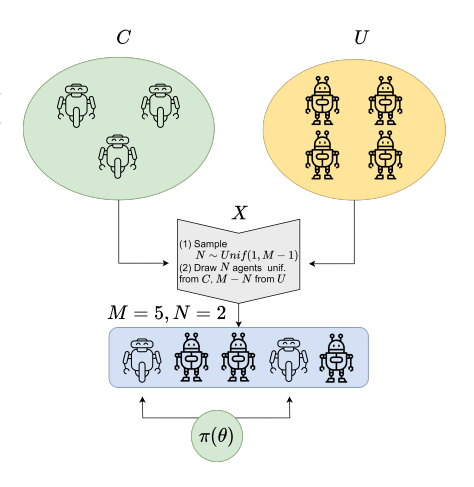
A.3 Experiment Details

A.3.1 Team Sampling Procedure Used in Experiments

Recall that U and C denote the sets of uncontrolled and controlled agent policies, respectively, while M denotes the total team size, and N the number of agents sampled from C. The experiments in the following consider an X_{train} consisting of sampling N uniformly from $\{1, \cdots, M-1\}$, sampling N agents from C and M-Nagents from U in a uniform fashion (Figure 7). The sampling procedure takes place at the beginning of each episode to select a team, which is then deployed in the environment. Data generated by the deployed team (e.g. joint observations, joint actions, and rewards) are returned to the learning algorithm. See Appendix A.3.3 for further details on the evaluation procedure.

A.3.2 Experimental Domains

MPE Predator Prey The MPE environment [23] (re- Figure 7: A practical instantiation of the leased under the MIT License) is a setting where particle agents interact within a bounded 2d plane, equipped with a discrete action space and continuous observation space. The observation space is 16-dimensional, and contains the



NAHT problem.

agents' own position and velocity, relative positions/velocities of all other agents, landmarks, and prey. The action space consists of 5 discrete actions, corresponding to the four cardinal movement directions and a no-op action.

The predator-prey task (mpe-pp) is a custom task implemented by the authors of this paper within the fork of the MPE environment released by Papoudakis et al. [29] (MIT License). In this task, three predators must cooperatively pursue a pre-trained prey agent. The team receives a reward of 1 if two or more predators collide with the prey at a single time step, and no reward if only a single agent collides with the prey. A shaping reward consisting of 0.01 times the ℓ_2 distance between each agents in the team and the prey is provided as well. The maximum episode length is 100 time steps.

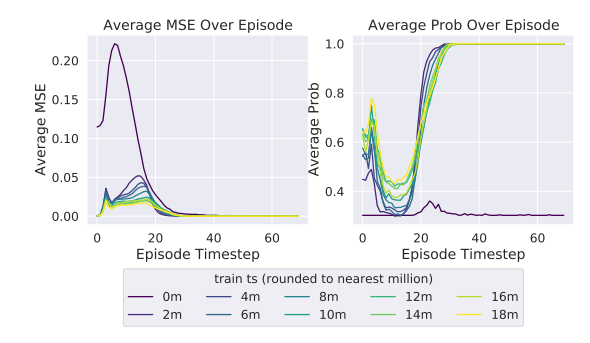
SMAC SMAC [33] (released under the MIT License) features a set of cooperative tasks, where a team of allied agents must defeat a team of enemy agents controlled by the game server. It is a partially observable domain with a continuous state space and discrete action space. For each agent, the observation space is continuous, and consists of features about itself, enemy, and allied agents within some radius. The action space is discrete, and allows an agent to choose an enemy to attack, a direction to move in, or to not perform any action. As the number of allies and enemies varies between tasks, the dimensionality of the observation and action spaces is particular to each task. The maximum number of time steps per episode is also task specific, although early termination occurs if all enemies are defeated. At each time step, the team receives a shaped reward corresponding to the damage dealt, and bonuses of 10 and 200 points for killing an enemy and winning the scenario by defeating all enemies. The reward is scaled such that the maximal return achievable in each task is 20.

The SMAC tasks considered in this paper are described in more detail below:

- 5v6: stands for 5m vs 6m, five allied Marines versus six enemy Marines.
- 8v9: stands for 8m vs 9m, eight allied Marines versus nine enemy Marines.
- 10v11: stands for 10m vs 11m, ten allied Marines versus eleven enemy Marines.
- 3s5z: stands for 3s vs 5z, three allied Stalkers versus five enemy Zealots.

A.3.3 Evaluation Details

The experiments in the main paper consider a particular team sampling procedure called X_{train} , which uniformly samples N and uniformly samples agents from the sets U and C. While the learning curves reported in the main paper are computed directly with X_{train} , we use an iterative and deterministic evaluation procedure for the results presented in Section 6.4 and in the Appendix. The purpose of the additional evaluation procedure presented here is to ensure that we thoroughly evaluate the trained NAHT agents for all possible values of N and all possible teammates.



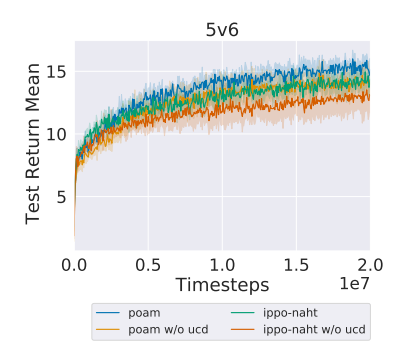


Figure 8: Evolution of the within-episode mean squared error (left) and probability of actions that were actually taken by modelled teammates (right), computed by the POAM agent over the course of training, on the 5v6 task. The agent modeling performance improves over the course of an episode, as more data about teammate behavior is observed.

Figure 9: Learning curves of POAM and IPPO, where the value network is trained with and without uncontrolled agents' data (UCD) on 5v6.

Given a set of uncontrolled agents U and a set of agents C generated by some NAHT method, we compute the following M-N cross-play scores. Let N be the number of agents sampled from C, such that N < M. For $N \in \{1, \cdots, M-1\}$, construct the joint policy $\pi^{(N)}$ by selecting N agents uniformly from C and M-N agents from U. Evaluate the resultant team on the task for E episodes. This results in M-1 episode returns, on which we may compute summary statistics. If agents in U and C are generated by algorithm A and B, respectively, then we call the thus computed average return, the M-N cross-play score.

More concretely: each algorithm (VDN, QMIX, QMIX-NS, IQL, IQL-NS) is run k times with different seeds, to generate k teams of teammates to act as uncontrolled agents. For each pair of algorithms, we sample a subset of the possible seed pairs, and evaluate the teams that result from merging said seed pairs. Note that each seed actually represents a team of agents. For example, if VDN and QMIX have seeds 1 2, and 3, the cross-play evaluation might consider the seed pairings (VDN 1, QMIX 2), (VDN 2, QMIX 3), (VDN 3, QMIX 1). Given a pair of seeds (e.g. (VDN 1), (QMIX 2)), the M-N cross-play score is computed as the average return generated by sweeping $N \in \{1, \cdots, M-1\}$ and evaluating the merged team that consists of selecting N agents from the first team, and M-N agents for E episodes. In our experiments, E=128, and k=3.

Means and standard errors are computed over all seed pairings considered, as we treat each M-N evaluation as an independent trial. For most experiments, three seed pairs are considered, where seeds are paired to ensure that all seeds participate in at least one evaluation. This ensures that the computational cost of the evaluation remains linear in k, rather than quadratic. However, note that for the OOD experiments presented in Section 6.4, we consider all possible seed pairings for the most comprehensive evaluation.

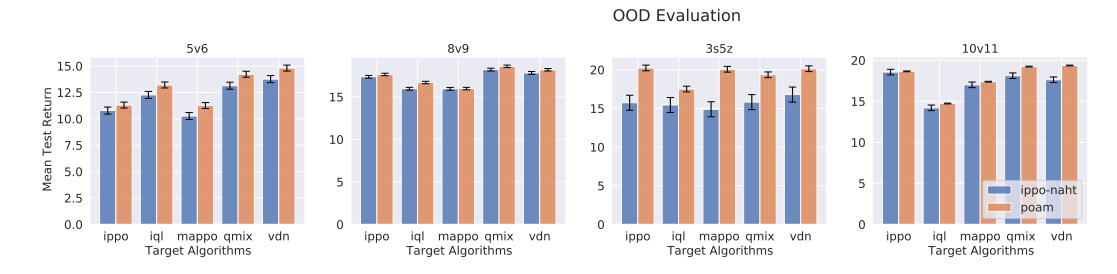


Figure 10: Mean and standard error of test returns achieved by POAM and IPPO-NAHT, when paired with out-of-distribution teammates. POAM shows improved generalization to OOD teammates, as compared to IPPO-NAHT, across all tasks.

Self-play scores. For algorithm pairs that *are* the same, seeds are paired with themselves. For example, the seed pairs for VDN versus VDN would be (1,1),(2,2),(3,3). The reason for this is that we are interested in the performance of agents when paired with known teammates. This is the *model* self-play score, in contrast to the *algorithm* self-play score [3].

A.3.4 Algorithm Implementation

The experiments in this paper use algorithm implementations from the ePyMARL codebase [29] (released under the Apache License). The value-based methods are used without modification (i.e. IQL, VDN, QMIX), but we implement our own version of policy gradient methods (IPPO, MAPPO), based on the implementation of [43].

All methods employ recurrent actors and critics, with full parameter sharing, i.e. all agents are controlled by the same policy, where the agent id is input to the policy/critic networks, to allow behavioral differentiation between agents. All methods employ the Adam optimizer to optimize all networks involved. For policy gradient methods, the policy architecture is two fully connected layers, followed by an RNN (GRU) layer, followed by an output layer. Each layer has 64 neurons with ReLU activation units, and employs layer normalization. The critic architecture is the same as the policy architecture. The value-based networks employ the same architecture, except that there is only a single fully connected layer before the RNN layers, and layer normalization is not used, following the ePyMARL implementation. Please consult the code base for full implementation details.

Hyperparameters. For the value-based methods, default hyperparameters are used. We tune the hyperparameters of the policy gradient methods on the 5v6 task, and apply those parameters directly to the remaining SMAC tasks. The hyperparameters considered for policy gradient algorithms are given in Table 1. POAM adopts the same hyperparameters as IPPO where applicable. We also tuned additional hyperparameters specific to POAM (see Table 2).

Algorithm	Buffer size	Epochs	Minibatches	Entropy	Clip	Clip value
						loss
IPPO	128, 256 , 512	1, 4, 10	1, 3	0.01, 0.03,	0.01, 0.05, 0.1	no, yes
				0.05		
MAPPO	64, 128, 256	4, 10	1, 3	0.01, 0.03 ,	0.05 , 0.1, 0.2	no, yes
				0.05, 0.07		-

Table 1: Hyperparameters evaluated for the policy gradient algorithms. Selected values are bolded

Task	Algorithm	ED epochs	ED Minibatches	ED LR
5v6	POAM	1 , 5, 10	1, 2	0.0005 , 0.005
mpe-pp	POAM	1, 5	1, 2	0.0005 , 0.001

Table 2: Additional hyperparameters evaluated for POAM; note that ED stands for encoder-decoder. Selected values are bolded.

A.4 Supplemental Results

A.4.1 Validating the Existence of Coordination Conventions

The experimental procedure detailed in Section 6.1 generates diverse teammates in SMAC and MPE by using MARL algorithms to train multiple teams of agents. Two underlying assumptions of the procedure are that (1) teams trained by the same algorithm learn non-compatible coordination conventions, and (2) teams trained by different algorithms are not compatible. Both points are experimentally verified in this section.

Self-play with MARL algorithms. For the tasks under consideration, teams trained using the same MARL algorithm, but different seeds, can converge to distinct coordination conventions. Figure 11 demonstrates this by depicting the return of teams trained together (matched seeds) versus those of teams that were not trained together (mismatched seeds), across all naive MARL algorithms (IPPO,

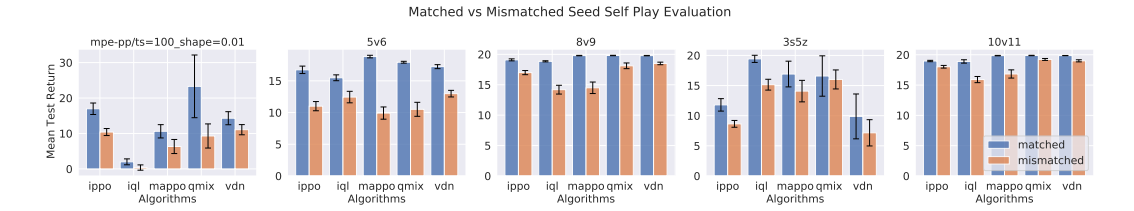


Figure 11: Agent teams that were trained together using the same algorithm (matched seeds) have higher returns than teams that were not trained together but were trained with the same algorithm (mismatched seeds).

IQL, MAPPO, QMIX, VDN) and tasks considered. Overall, the returns of the teams that were trained together are higher than those not trained together.

The general phenomenon has been previously observed and exploited by prior works in ad hoc teamwork [38]. This paper takes advantage of this to generate a set of diverse teammates for the StarCraft II experiments. We select tasks where the effect is significant, to ensure that there are distinct coordination behaviors for POAM to model. Tasks that were considered but subsequently ruled out for this reason include 3m vs 3m, 8m vs 8m, 6h vs 8z, and the MPE Spread task.

Cross-play with MARL algorithms Tables 12, 13, 14, 15, and 16 display the full cross-play results for all MARL algorithms on all tasks. Note that the tables are reflected across the diagonal axis for viewing ease. The values on the off-diagonal (i.e., where the two algorithms are not the same) are the cross-play score, while the values shown on the diagonal are self-play scores, computed as described in App. A.3.3. The cross-play and self-play scores displayed are means and *standard errors*. The rightmost column reflects the row average and *standard deviation* of the cross-play (xp) scores corresponding to the test set of VDN, QMIX, IQL, IPPO, and MAPPO, excluding the self-play score. Thus, the rightmost column reflects how well on average the row algorithm can generalize to unfamiliar teams.

Overall, we find that MARL algorithms perform significantly better in self-play than cross-play. We note that there are a few exceptions (e.g., IPPO vs QMIX on 8m), and that the cross-play and self-play scores are much closer on 10v11, but overall the trend is consistent across tasks.

	vdn	qmix	iql	ippo	mappo	poam-aht	mean xp score
vdn	14.305 +/- (1.844)	8.657 +/- (2.925)	4.423 +/- (1.677)	2.374 +/- (0.730)	1.912 +/- (1.394)	8.101 +/- (1.164)	4.342 +/- (1.244)
qmix	8.657 +/- (2.925)	23.297 +/- (8.845)	3.359 +/- (1.691)	2.692 +/- (1.522)	2.691 +/- (1.365)	10.287 +/- (1.297)	4.350 +/- (1.255)
iql	4.423 +/- (1.677)	3.359 +/- (1.691)	1.997 +/- (0.835)	1.520 +/- (0.820)	0.325 +/- (0.552)	4.809 +/- (1.924)	2.407 +/- (0.811)
ippo	2.374 +/- (0.730)	2.692 +/- (1.522)	1.520 +/- (0.820)	16.974 +/- (1.621)	8.776 +/- (1.244)	13.584 +/- (1.412)	3.840 +/- (1.056)
mappo	1.912 +/- (1.394)	2.691 +/- (1.365)	0.325 +/- (0.552)	8.776 +/- (1.244)	10.616 +/- (1.874)	8.809 +/- (2.012)	3.426 +/- (1.157)
poam-aht	8.101 +/- (1.164)	10.287 +/- (1.297)	4.809 +/- (1.924)	13.584 +/- (1.412)	8.809 +/- (2.012)		9.118 +/- (1.068)

Figure 12: Cross-play table for the mpe-pp task.

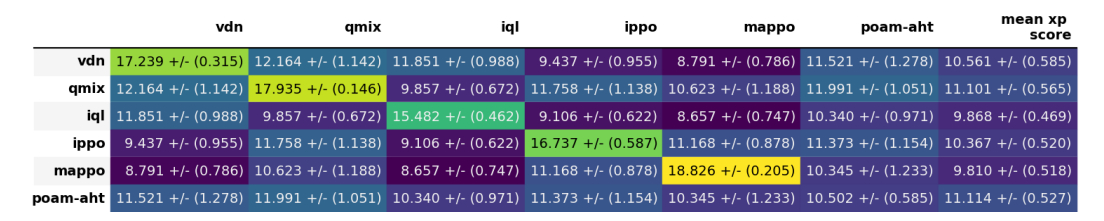


Figure 13: Cross-play table for the 5v6 task.

A.5 Cross-play performance as a function of the number of agents.

To provide more insight on how a non-NAHT team performance changes as the number of unseen agents increases, Figure 17 plots QMIX and IPPO's test scores on 5v6 when paired with various

	vdn	qmix	iql	ippo	mappo	poam-aht	mean xp score
vdn	19.788 +/- (0.036)	18.631 +/- (0.207)	15.520 +/- (0.838)	16.899 +/- (0.571)	14.999 +/- (0.952)	14.330 +/- (1.002)	16.512 +/- (0.422)
qmix	18.631 +/- (0.207)	19.811 +/- (0.035)	15.754 +/- (0.819)		15.338 +/- (0.799)	14.815 +/- (1.004)	16.828 +/- (0.385)
iql	15.520 +/- (0.838)	15.754 +/- (0.819)	18.854 +/- (0.093)	14.229 +/- (0.863)	12.995 +/- (0.878)	13.053 +/- (0.953)	14.625 +/- (0.463)
ippo	16.899 +/- (0.571)		14.229 +/- (0.863)	19.093 +/- (0.163)	15.390 +/- (0.825)	15.197 +/- (0.922)	16.027 +/- (0.413)
mappo	14.999 +/- (0.952)	15.338 +/- (0.799)	12.995 +/- (0.878)	15.390 +/- (0.825)	19.795 +/- (0.037)	13.965 +/- (0.999)	14.680 +/- (0.462)
poam-aht	14.330 +/- (1.002)	14.815 +/- (1.004)	13.053 +/- (0.953)	15.197 +/- (0.922)	13.965 +/- (0.999)	12.370 +/- (0.469)	14.272 +/- (0.450)

Figure 14: Cross-play table for the 8m task.

	vdn	qmix	iql	ippo	тарро	poam-aht	mean xp score
vdn	9.879 +/- (3.722)	13.742 +/- (3.270)	13.345 +/- (2.114)	8.061 +/- (1.981)	8.689 +/- (1.618)	19.367 +/- (0.601)	10.959 +/- (1.416)
qmix	13.742 +/- (3.270)		15.780 +/- (2.290)	11.130 +/- (3.400)	14.541 +/- (2.466)	19.333 +/- (0.814)	13.798 +/- (1.542)
iql	13.345 +/- (2.114)		19.429 +/- (0.594)	12.757 +/- (1.224)	11.704 +/- (1.275)	17.131 +/- (0.895)	13.397 +/- (1.009)
ippo	8.061 +/- (1.981)	11.130 +/- (3.400)	12.757 +/- (1.224)	11.794 +/- (1.034)	11.291 +/- (1.297)	19.609 +/- (1.080)	10.810 +/- (1.203)
mappo	8.689 +/- (1.618)	14.541 +/- (2.466)	11.704 +/- (1.275)	11.291 +/- (1.297)	16.910 +/- (2.133)	20.257 +/- (0.793)	11.556 +/- (1.079)
poam-aht	19.367 +/- (0.601)	19.333 +/- (0.814)	17.131 +/- (0.895)	19.609 +/- (1.080)	20.257 +/- (0.793)	20.172 +/- (0.579)	19.139 +/- (0.480)

Figure 15: Cross-play table for the 3s5z task.

methods, as a function of the number of unseen agents. Note that k=0 corresponds to teams entirely composed of the evaluated agents, while k=5 corresponds to teams entirely composed of the unseen teammates, and are actually self-play scores, whereas the other points are cross-play scores. These points appear on the plot to contextualize the performance of the mixed teams.

QMIX and IPPO have similar returns in self-play, but comparing the two figures, we observe a difference in the rate at which the cross-play returns decline. In particular, QMIX's performance declines most around k=3 across a variety of methods, while IPPO's performance is minimized at k=2.

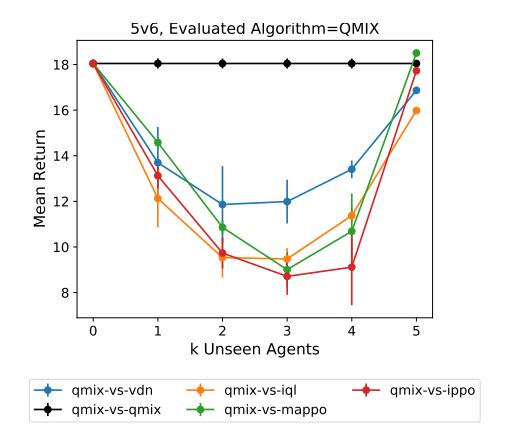
A.6 Computing Infrastructure

All value-based algorithms (e.g. QMIX, VDN, IQL) were run without parallelizing environments, while policy gradient algorithms were run with parallelized environments. All methods were trained for 20M steps on all tasks. Each run took between 12-48 hours of compute, and used less than 2gB of GPU memory. Runs were parallelized to use computational resources most efficiently. The servers used in our experiments ran Ubuntu 18.04 with the following configurations:

- Intel Xeon CPU E5-2630 v4; Nvidia Titan V GPU.
- Intel Xeon CPU E5-2698 v4; Nvidia Tesla V100-SXM2 GPU.
- Intel Xeon Gold 6342 CPU; Nvidia A40 GPU.
- Intel Xeon Gold 6342 CPU; Nvidia A100 Gpu.

	vdn	qmix	iql	ippo	mappo	poam-aht	mean xp score
vdn	19.868 +/- (0.021)	18.980 +/- (0.260)	18.276 +/- (0.274)	18.638 +/- (0.197)	16.453 +/- (0.864)	16.328 +/- (0.714)	18.087 +/- (0.280)
qmix	18.980 +/- (0.260)	19.884 +/- (0.034)		18.193 +/- (0.311)	18.608 +/- (0.370)	16.395 +/- (0.684)	18.282 +/- (0.199)
iql	18.276 +/- (0.274)		18.901 +/- (0.279)	16.610 +/- (0.547)	16.206 +/- (0.692)	14.826 +/- (0.650)	17.110 +/- (0.282)
ippo	18.638 +/- (0.197)	18.193 +/- (0.311)	16.610 +/- (0.547)	18.971 +/- (0.112)		16.125 +/- (0.566)	17.622 +/- (0.247)
mappo	16.453 +/- (0.864)	18.608 +/- (0.370)	16.206 +/- (0.692)		19.862 +/- (0.039)	15.670 +/- (0.708)	17.079 +/- (0.351)
poam-aht	16.328 +/- (0.714)	16.395 +/- (0.684)	14.826 +/- (0.650)	16.125 +/- (0.566)	15.670 +/- (0.708)	12.179 +/- (0.151)	15.869 +/- (0.308)

Figure 16: Cross-play table for the 10v11 task.



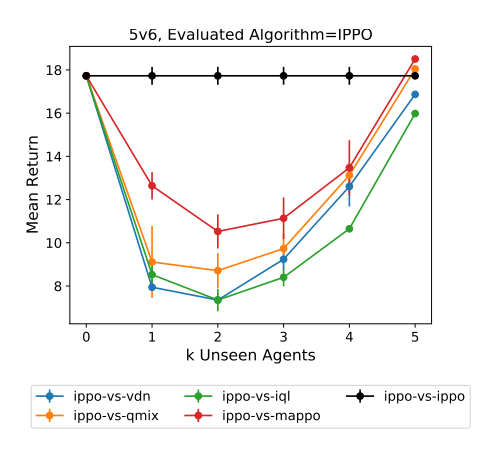


Figure 17: Mean and std. error of QMIX (left) and IPPO (right) test returns on 5v6, in the presence of uncontrolled agents generated by various MARL learning algorithms, as the number of unseen agents increases from k=0 to a maximum of k=5. The unseen agents are generated by the second method in the legend name.